CEBAF Program Advisory Committee Six (PAC6) Proposal Cover Sheet

This proposal must be received by close of business on April 5, 1993 at :

CEBAF
User Liaison Office
12000 Jefferson Avenue
Newport News, VA 23606

Proposal Title

Determination of four structure functions of the kaon electroproduction processes

Contact Person

Name : S. Frullani

Institution : Physics Laboratory, I.S.S. and INFN Sezione Sanità

Address : Viale Regina Elena 299

Address :

City, State ZIP/Country : Rome, Italy 00161

Phone : + 396 4990 ext 235 **FAX : + 396 446 2872**

E-Mail BITnet : **Internet : Frullani @ ISS.INFN.IT**

If this proposal is based on a previously submitted proposal or letter-of-intent, give the number, title and date :

CEBAF Use Only

Receipt Date : 4/5/93 Log Number Assigned : PR 93-047

By : gf

Determination of four structure functions of the kaon electroproduction processe

E.Cisbani, S. Frullani (Spokesman), F. Garibaldi , M. Jodice, G.M. Urciuoli
Physics Laboratory, Istituto Superiore di Sanità and INFN Sezione Sanità, Rome, Italy
R. De Leo, R. Perrino
Physics Department, Università di Lecce and INFN Sezione Lecce, Lecce, Italy
M. Sotona
Nuclear Physics Institute , 25068 Rez/Prague, Czech Republic
G.G. Petratos
SLAC, Stanford University, Stanford, CA 94300 *
G.M. Huber, G.J. Lolos
University of Regina, Canada
C.F.Perdrisat and collaborators
(Phys. Dept. College of William and Mary, Williamsburg, Va 23185)
Vina Punjabi and students
(Dept. of Phys. and Chem. Norfolk StateUniversity,Norfolk, Va 23504)

and

MPS Collaboration

* SLAC is not sponsoring this initiative as an Istitution, given its policy of only supporting research activities at SLAC. The participation of G.G.Petratos is possible because of his fixed term research appointment at SLAC.

ABSTRACT

Measurements of the four response functions of the kaon electroproduction processes on Λ and Σ channels could give an important contribution in the comprehension of strangeness production. The current experimental knowledge, coming from data taken with low duty cycle and low intensity beams, is insatisfactory. No systematic separation of different contributions has been attempted. Many models, sometimes with a large number of parameters, try to explain existing data. We propose to measure the separate structure functions in different kinematical regions with three different aims. The first is to provide measurements of the basic electroproduction process in kinematical conditions common to those of the proposed experiments for high resolution hypernuclear studies , the second is to perform measurements in kinematical conditions optimized to try to approach the problems connected with the determination of the electromagnetic kaon form factor through the electroproduction reaction, the third is to measure the angular distribution in kinematical conditions that include also the transition to a regime in which the theoretical approach based on diquarks description of the elementary process could be applicable. The proposed MPS spectrometer, with its capability of small forward scattering angle and out-of-plane set-up, can provide high quality measurements.

1. Introduction

The current situation for kaon photo- and electroproduction is somewhat unsatisfactory, both from the experimental and theoretical point of view. Measurements of the $\gamma + p \Longrightarrow K^+ + Y$ and $e + p \Longrightarrow e' + K^+ + Y$ ($Y = \Lambda, \Sigma$) reactions have been limited by short lifetimes ($c.\tau_K = 370$ cm, $c.\tau_\Lambda = 8$ cm), small production rate (roughly by one order of magnitude compared with pions) and high thresholds ($E_t(K\Lambda)= 911$ MeV, $E_t(K\Sigma)= 1.05$ GeV). The present photoproduction data (reviewed, e.g. , in ref. [1]) are not much better than twenty years ago. The cross sections are known with an accuracy of about 10%. The polarizations are determined only for few points in the Λ production with large errors from 25% to 50%. The photon energy range is limited to $0.9<E_\gamma<1.4$ GeV (few other points were measured [2] for the fixed momentum transfer $t = -0.147$ GeV^2 in the energy range $E_\gamma= 1.05 - 2.2$ GeV). Electroproduction data are also sparse and measured only at higher energies (virtual photon-proton center of mass energy $W> 2.1$ GeV). The experimental information on Σ^0 production is even more scarce. In the following we will focus on the Λ production but all our proposed measurements on the proton will allow the measurement at the same time of the Σ channel.

There are also deep and important theoretical problems in our understanding of the process. In the low energy region various semiphenomenological descriptions in terms of mesons and baryons are used. The hadronic field theories do not explicitly contain the quark degrees of freedom, but they provide a suitable effective scheme for description of dynamics in a low- and intermediate-energy range. The semiphenomenological parameters of the theory (strong coupling constants, transition magnetic moments) are fitted to the photoproduction data available, making use of the transition amplitude based on the tree level Feynman diagrams (Fig 1).

In general, phenomenological χ^2 parameter fits are not unique due to a large number of the coupling constants (up to 12 effective parameters are used; four of them are entering the Born terms and the rest is associated with the resonance terms [3]) and due to the large experimental errors in the data. Hence, many sets of the parameters can fit the data equally well in the photoproduction channel. The various fits may, however, differ significantly when extrapolated outside the kinematics used in the fitting procedure ($E_\gamma>1.4$ GeV, virtual photons). They are also not equivalent from the point of view of the theoretical interpretation.

First of all there is a serious disagreement between the values of coupling constants derived from the purely hadronic processes and from the available photoproduction data. The value of the leading coupling constant $g_{K\Lambda p}/\sqrt{4\pi}$ is in the range from -1 to -3 in most photoproduction models, while its accepted hadronic value is about -4 [4], in agreement with the broken SU(3) prediction [1]. This discrepancy can be resolved by inclusion of the t-channel K_1 resonance state with $J=1^+$ ($M=1280$ MeV, $\Gamma=90$ MeV) but only at the price of a very strong $K_1\Lambda p$ coupling [1,5].

Due to the same reasons (the lack of high quality experimental data in appropriate kinematical region), all attempts to investigate the problem of electromagnetic production of strangeness on subnucleon (quark) level are at the very begining. Only recently [6,7] the description of the photo- electroproduction reaction in terms of the hard scattering model of Brodsky and Lepage and of the diquark mechanism has been tried.

Thus, the situation in the theory of photo- and electroproduction of strange mesons is rather complicated. A lot of models were constructed (see e.g. review in [8]) that differ in a number and choice of contributing resonances as well as in the fitted coupling constants (including the leading ones $g_{K\Lambda p}$ and $g_{K\Sigma p}$). On the other hand, the available experimental data on the photoproduction cross sections are explained (i.e., fitted) by these models equally well - Fig. 2.The Λ polarization data are more selective in this respect. Here predictions of various models differ significantly - Fig. 3. Nevertheless, the experimental points are so sparse and the error bars so large that only the models based on the Born diagrams alone can be rejected unambiguously [8].

It is clear, that new precise measurement of the production cross- sections and Λ polarization will be of large importance for better understanding of the process of electromagnetic production of strangeness. The electroproduction cross-section for unpolarized particles in the initial state (electron and proton) is determined by 4 response functions [9]: transverse R_T, longitudinal R_L, transverse-longitudinal interference term R_{TL} and transverse-transverse interference term R_{TT}. The last two terms are multiplied in the expression of the cross section by $\cos\alpha$ and $\cos 2\alpha$ respectively (being α the angle between scattering and production planes), and due to this simple dependence they can be easily separated from the cross section if noncoplanar measurements are possible. The remaining part of the photoproduction cross-section (by virtual photons) is then given in the centre-of-mas system by

$$d\sigma_U/d\Omega_K=|q_K|/|k_\gamma| \cdot \{R_T + \varepsilon_L . R_L\} \qquad (1)$$

where q_k and k_γ are the momentum of kaon and virtual photon in the laboratory system.
σ_U may be, in principle, further divided into the transverse and longitudinal parts R_T and R_L as far as the cross-section is measured at two different values of virtual photon polarization ε ($\varepsilon_L = (Q^2/E_\gamma^2).\varepsilon$). The measurement of the separated four structure functions gives much more constraints to a satisfactory theoretical description of the reaction. For this purpose for a given value of W (total energy of the initial or final system), $q\mu$ (4-momentum of the virtual photon) and t (4-momentum transfer to the hyperon, linearly connected with the angle between the emitted kaon and the 3-momentum of the virtual photon), that are the variables on which the four structure functions depend, four independent measurements of cross sections are required to carry out the separation. For the special case in which the kaon is detected in the same direction of the virtual photon the two interference terms are zero and only two measurements at two

different values of the virtual photon polarization parameter are required to separate the longitudinal and transverse terms.

2. Physics motivations of the proposed measurements

We propose to measure the separate structure functions in different kinematical regions with three different aims. The first is to provide measurements of the basic electroproduction process in kinematical conditions common to those of the proposed experiments for high resolution hypernuclear studies [10], the second is to perform measurements in kinematical conditions optimized to try to approach the problems connected with the determination of the electromagnetic kaon form factor through the electroproduction reaction, the third is to measure the angular distribution in kinematical conditions that include also the transition to a regime in which the theoretical approach based on diquarks description of the elementary process could be applicable.

a) Hypernuclear kinematics.

The mechanism of formation of an hypernuclear system involves on one hand the process of electroproduction and on the other hand the process of the transition from the target ground state to the hypernucleus. The population of the different final hypernuclear states depends both on their coupling to the initial state of the target nucleus and on the strength of the appropriate electromagnetic multipoles, needed to allow the transition, in the electroproduction process.

TABLE 1

	AB2	AS1	AS2	AW1	AW2	TH2	W1	C1	C2
$J=1^-$	20.3	28.3	24.9	22.3	28.8	23.7	21.3	20.3	29.7
$J=2^-$	64.3	101.9	106.1	74.7	92.9	78.3	68.6	75.7	92.4
long. %	5.0	16.5	29.5	10.5	6.9	9.2	6.9	19.6	3.5
$J=3^+$	78.2	125.5	132.7	91.3	113.1	95.5	83.4	93.5	111.9
long.%	5.7	18.25	32.0	11.7	7.6	10.3	14.8	21.5	3.9

AB2 [11], AS1,AS2[1], AW1,AW2[5], TH2[12], W1[13], C1,C2[3]

In Table 1 the cross sections (nb/sr) for the $^{12}C(e,e'k^+)^{12}B_\Lambda$ reaction leading to different hypernuclear states are reported for some of the proposed models of the electroproduction process used in the theoretical description of the reaction. In all the cases the nuclear ingredients

are the same. One can see that the absolute strengths of the different levels as well as their ratio can differ in an appreciable way and that the knowledge of the amplitudes of the elementary k-Λ production on the proton at the same value of the relevant kinematical variables is necessary to disentangle as much as possible different ingredients that enter in the description of the full process.

In Table 1 for the transition to the 2- and 3+ levels are also reported the percentage of the cross section that, according to the different models, is due to longitudinal polarized virtual photons (the transition to the 1^- level has a pure transverse character). One can see how this component changes to confirm how it is important also to measure the separate structure functions.

b) Kinematics to approach the determination of kaon form factor.

The knowledge of the electromagnetic structure of any complex particle , made of charged substructures, has been always a fundamental milestone in the comprehension of its structure in terms of behaviour of the more fundamental components. The electromagnetic form factor is certainly the quantity that more easily can be theoretically deduced from models describing the way in which elementary components behave when they aggregate to form complex structures. It depends only on the square of the four-momentum transfer to the particle by the electromagnetic probe. Electron-positron colliding-beam experiments measure the form factor in the time like region generally via the production of a pair of particle-antiparticle. However the experimental measurement of particle form factor in space like region is straightforward only for the case of nucleons as they can be used as free targets, indeed only in this case, as it is for time like electroproduction, the cross sections are directly proportional to the absolute square of the form factor. For particles (mesons and baryons) that can be produced in sufficient quantity to be used as secondary beams in large hadron accelerators, their scattering on atomic electrons can give a measurement of the form factor but, due to the small electron mass, only low values of momentum transfer can be obtained. At large space like momentum transfers the only reactions that can give information on form factors is the electroproduction process from nucleons and this implies that the possible determination of form factor is in any case model dependent due to the competition of many interfering processes contributing to the electroproduction reaction in addition to the one of interest in which the electromagnetic probe interacts directly with the produced particle. The extraction of the form factor from the data requires a big effort both from the experimental and theoretical side. A great effort has been spent in the seventies [14,15] to determine the pion form factor .

For the kaon in space like region the only existing measurements come from k-e scattering [16,17] and are limited to a value of 4-momentum transfer of 0.1 $(GeV/c)^2$. The possibility to determine the kaon form factor through the electroproduction reaction relies on the fact that the t

diagram of fig 1c, in which the meson exchanged is the kaon (kaon pole diagram), overwhelms the contribution of all the other diagrams near the unphysical value of the t variable $t=m_K^2$ and on the hope that this behaviour is enough strong to influence the cross section also at physical values of t allowing a smooth extrapolation from experimental points to $t=m_K^2$. The effort that one should expect from the theoretical side is to have guidance in extrapolation techniques exploiting model-independent constraints and analytical properties of amplitudes. From experimental side one has to provide measurements as precise as possible in kinematical conditions that are more favourable to allow the extrapolation. For a given q_μ^2 and a given W there is a minimum value for the variable -t in the physical region (t_{min}) that corresponds to the kinematical condition in which the kaon is emitted in the same direction of the 3-momentum transfer. In fig 4 the dependence of t_{min} from W for different values of q_μ^2 is shown, a good choice of kinematical conditions should allow to reach a small value of t_{min} in order to be in the best condition to perform the extrapolation. We want measure the four structure functions at three values of $\{q_\mu^2$ (GeV/c)^2, W (GeV)$\}$ pair : { -0.1, 2.1 } , { -0.3, 2.2} and { -0.5, 2.2 } for four t values up to the minimum (absolute) value allowed that it is 0.054, 0.075 and 0.107 respectively. These are the best conditions due the maximum beam energy (6 GeV assumed) and the maximum kaon momentum measurable by MPS (we assume in this proposal the version of MPS at 2.0 Gev/c maximum central momentum [18]) and are also good conditions in absolute sense because the minimum t value attained is not too far from what it is reachable at a much higher value of W (see fig 4). For the considered values of 4-momentum transfer the use of small forward angle capability is important both to reach t_{min} conditions and to optimaze the separation of longitudinal-transverse parts.

The observable to extrapolate can be the longitudinal response function or the sum of longitudinal and transverse part shown in (1) or even the full cross section provided that the TL interference term has been removed or has been demonstrated to be negligible [14]. In this regard one has to consider that to eliminate the TL term, the usual procedure to perform measurements on scattering plane at two symmetric angles respect to the virtual photon direction is not applicable and one has to use necessarily out-of-plane capability.

The available until now electroproduction data do not allow to realize such procedure and it is not incomprehensible that from the theoretical side practically no activity has been specifically devoted to the problems connected with the possible derivation of kaon form factor from experimental data.

We have tried to see what would be the situation if the experimental points available were according to different models. The cross section σ_U (1) for the kaon-pole diagram is given by :

$$R_T+\varepsilon_L.R_L=\text{const}\,.(g_{K\Lambda N})^2/s\,\{-t+(m_\Lambda-m_p)^2\}.$$

$$\{k_f^2.\sin^2\Theta_K/2 + \varepsilon.(e_K.k_i - e_\gamma.k_f.\cos\Theta_K)^2/Q^2\}.F_K(Q^2,t)/(t-m_K^2)^2. \qquad (2)$$

being k_i, k_f the initial and final state momentum of the particles in cm system, e_K and e_γ the energy of the kaon and the virtual photon in the same system, Θ_K the angle of the emitted kaon and $Q^2 = -q\mu^2$.

If this term dominates the cross section σ_U at small t then there is a hope that the kaon form factor $F_K(Q^2) = F_K(Q^2, t=m_K^2)$ may be extracted from (1) by extrapolation to $t=m_K^2$. For some phenomenological models of photo- and electroproduction the situation is illustrated in Figs. 5 - 9. The calculated σ_U are divided by the asymptotic expression (2). At the kaon pole the value of the "renormalized" cross-section thus should be exactly equal 1 - this point is also shown in the figures by a corresponding asterisk at $t=m_K^2 \approx 0.24$ GeV^2.

At smaller energies (w=2 GeV, Fig. 5-6) it is seen that from the behaviour of different models up to $t = t_{min}$ it is hard to believe that such extrapolation of "real" electroproduction data (reproducing any of the models) would be successful. At higher energy (w=3 GeV, Fig. 7-9) the situation seems to be better (at least for some models), especially at higher values of Q^2.
What the figures show is not more than the visualization of the weight in different models of the kaon pole term, but they could give also an encouraging message. All the models have been adjusted on low energy photoproduction data, some ones (those that seem to have a smoother behaviour) on medium energy electroproduction data as well. There is an evident lack of new good quality data.

Similar a priory "theoretical" analysis of the problem of kaon form factor is a little risky of course and one has to confront with real experimental data. Anyhow, the high quality experimental data on low- and intermediate virtual photon energy, allowing the determination of separate response functions would be of large interest. They would enable to distinguish easily between different photo- and electroproduction models and, may be, they will shed a new light on the problem of kaon form factor as well.

c) Large t kinematics.

The study of exclusive reaction at large t provides a way to shed some light in the interaction mechanism which occur at short distance in hadronic matter, selecting an hard mechanism regime of the reaction in comparison with a diffractive mechanism that occurs at small t values.

In these last years theoretical predictions of exclusive photo-electroproduction reactions based on perturbative QCD [6] or on QCD inspired semiphenomenological diquark model [7] have become available. In Fig 10 the experimental data of high energy (4 and 6 GeV) Λ photoproduction reaction together with the predictions of the two models are shown. The kinematical region in which computations based on the diquark approach are considered to be applicable is well within CEBAF capability (W > 2 GeV) and one has only to measure the angular distribution including large enough values of t (< -1.5 (GeV/c)^2), allowing in this way a

transition between small and large t where different descriptions of the reaction should be applicable. Also in this case the possibility to separate the four response functions is useful to compare more observables with the theory and to give guidance if some discrepancy is found. To have the possibility to separate the structure function at large t values an out-of-plane capability with important vertical raising angle Φ_k is necessary.

3. Kinematical conditions and counting rates

In tables 2-19 we report the kinematical and experimental conditions considered, for different (Q^2,W,t) kinematics, for the complete separation of the four response functions which contribute to the total cross sections of the elementary electroproduction process p(e,e'k): σT, σL, σP, σI.

Cross sections, counting rates and statistical accuracy for the measured and separated structure functions have been all estimated on the basis of the same model (C1 of ref. [3]) so that the estimated accuracy obtained with the foreseen measurements in the extraction of the separated response functions could be different according to other models.

The single electron arm counting rates are computed with an extension of the QFS code of Lightbody and O'Connel [20] allowing to compute (e,e') cross sections on protons target. Protons and pions single rates have been also computed with the EPC code of the same authors while, for the single kaon rates the procedures suggested in ref. [21] have been adopted. For this last case an alternative procedure have been also used, consisting in the integration of the coincidence p(e,e'K) cross section with respect to the scattered electron free kinematical variables. With this method the computed single kaon rates differ, in excess, for about one order of magnitude with respect to the mentioned previous procedure. In any case, due to the low accidental coincidence rates, this does not influence the times of the measurements.

On the other hand it is important to consider the high protons and pions rates that have to be supported by the kaon spectrometer. Backgrounds up to 5 10^7 protons/sec have to be considered working at forward angles, which implies

a careful design of the detection system and an accurate choice of the associated electronic devices.

In tables 2,3 we report the kinematics at Q^2=-0.1GeV^2 and W=1.9 GeV chosen to investigate the typical kinematical conditions adopted for hypernuclear studies, as explained in chapter a. Connected with the studies on the kaon form factor, are the kinematics reported in tables 4-15 for Q^2 = 0.1, 0.3 and 0.5 GeV^2 and, at last, large t kinematics are reported in tables 16-19.

For all these kinematics the experimental conditions are the same here reported:

Kinematical conditions

electron momentum acceptance	$\Delta E/E$	= +/- 5 %
electron solid angle	$\Delta\Omega$	= 2 msr
kaon momentum acceptance	$\Delta P/P$	= +/- 7.5 %
kaon solid angle	$\Delta\Omega$	= 10 msr
Luminosity	L	= $2.\ 10^{37}$
kaon survival probability	f	= from 30 % to 50 % according to the kaon momenta

In the case of the "low ε" kinematics proposed at $Q^2 = 0.3$ GeV^2 and $Q^2 = 0.5$ GeV^2, as well as for all the kinematics chosen at $Q^2 = 1.0$ GeV^2, a different setup for the HRS spectrometer, always working with the septum magnet for forward angles detection, has been considered. It allows to increase its solid angle up to its normal value of 7.8 msr and hence the counting rates are consequently increased. This is possible in such kinematics, due to the angle of the scattered electron that never goes below 12° which gives a condition of "non-interference" between the electron and kaon spectrometer as considered in the set up for forward measurement in ref. [19]

The beam time requirements are also reported in the tables and are here summarized:

Beam time required for "typical Hypernuclear conditions"	49 hours
Beam time required for "kaon form factor investigations"	368 hours
Beam time required for "large t kinematics"	296 hours

A total of 1000 hours are therefore needed for all the measurements having included about a factor of 40 % to take into account calibration, variation of kinematical conditions and contingency.

References

[1] Adelseck R.A. and Saghai B.: Phys. Rev. C 42(1990) 108

[2] Feller P. et al.: Nucl. Phys. B39 (1972) 413

[3] Williams R., Ji Ch.-R., and Cotanch S.R.: Phys. Rev. D41 (1990) 1449

[4] Dover C.B. and Walker G.E.: Phys. Rep. 89 (1982) 1

[5] Adelseck R.A. and Wright L.E.: Phys. Rev. C38 (1988) 1965

[6] Farrar G. R., Huleihel K. and Zhang H.: Nucl. Phys. B349 (1991)655

[7] Schuermann M., 1992, Thesis, Wuppertal University

[8] Adam J., Mares J., Richter O., Sotona M., and Frullani S.:Czech. J. Phys. 42 (1992) 1167

[9] Drechsel D. and Tiator L.: J. Phys. G 8 (1992) 449

[10] Saito T. et al., High Resolution Electroproduction of Light Hypernuclei, Proposal submitted to PAC6

Frullani S. et al., High Resolution 1p shell Hypernuclear Spectroscopy, Proposal submitted to PAC6

[11] Adelseck R.A., Bennhold C. and Wright L.E.: Phys.Rev. C 32(1985) 1681

[12] Thom H.: Phys.Rev. 151 (1966) 1322

[13] Workman R.L.: Phys.Rev. C44 (1991) 552

[14] Devenish R.C.E. and Lyth D.H.: Phys.Rev. D5 (1972) 47

[15] Bebek C.J. et al. : Phys.Rev. D7 (1978) 1693

[16] Dally E.B. et al. : Phys.Rev.Lett. 45 (1980) 232

[17] Amendolia S.R. et al. : Phys.Lett. B (1986) 435

[18] The MPS project with 2 GeV/c has been evolved from the original project [19] and presented in the meeting held at CEBAF in March 1992.

[19] S.Frullani, F.Garibaldi, F.Ghio, M.Jodice, G.M.Urciuoli, R.De Leo, Multi Purpose Spectrometer, I.N.F.N. - I.S.S. 90/5, July 1990

[20] J.W.Lightbody Jr., J.S.O'Connel, Comp.in Physics, May/June 1988, p.57

[21] C.E. Hyde-Wright, W.Bertozzi, J.M.Finn Proc. of the 1985 CEBAF Workshop.

Figure captions

Fig. 1. Tree Feynmam diagrams used to describe the kaon electroproduction process in the semiphenomenological description in terms of mesons and baryons. B stands for proton or strangeness nucleon resonances; S stands for baryon with strangeness S = -1 and M for mesons.

Fig. 2. Photoproduction cross section calculated with different models.

Fig. 3. The experimental Λ-polarizations in the photoproduction of kaon compared with some model prediction.

Fig. 4. Locii of the minimum (in absolute value) t reachable in the physical region for given W and 4-momentum squared. Each curve refers to a constant Q^2 value shows in the figure.

Fig 5. - Fig 9 . Ratio of su (see text) predicted by different models to the same cross section given by the only contribution of the kaon pole graph in different kinematical conditions.

Fig 10. Comparison of photoproduction data obtained at energy of 4 and 6 GeV with model predictions based on: a) perturbative QCD [6] and b) diquarks model [7] both assuming an hard scattering process.

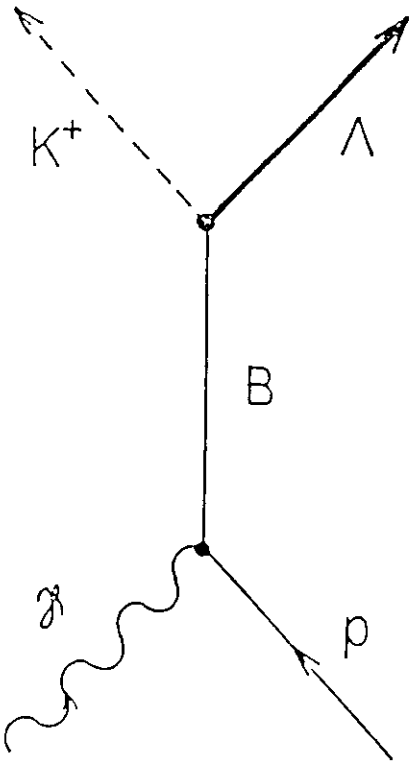

S.- CHANNEL

a)

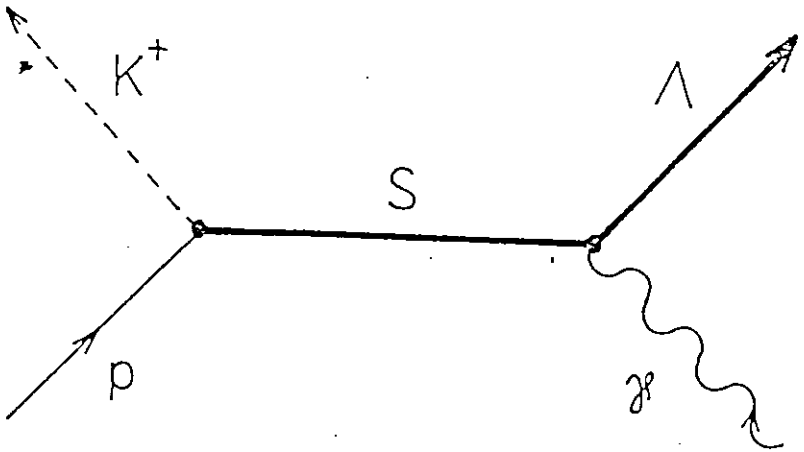

U - CHANNEL

b)

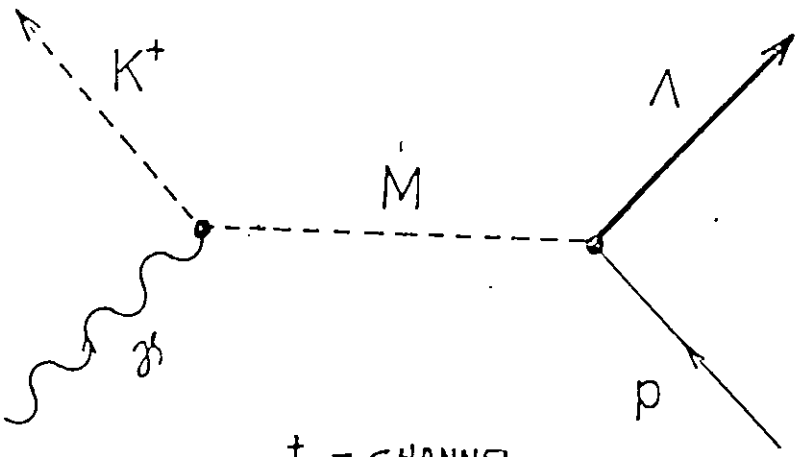

t.- CHANNEL

c)

FIG. 1

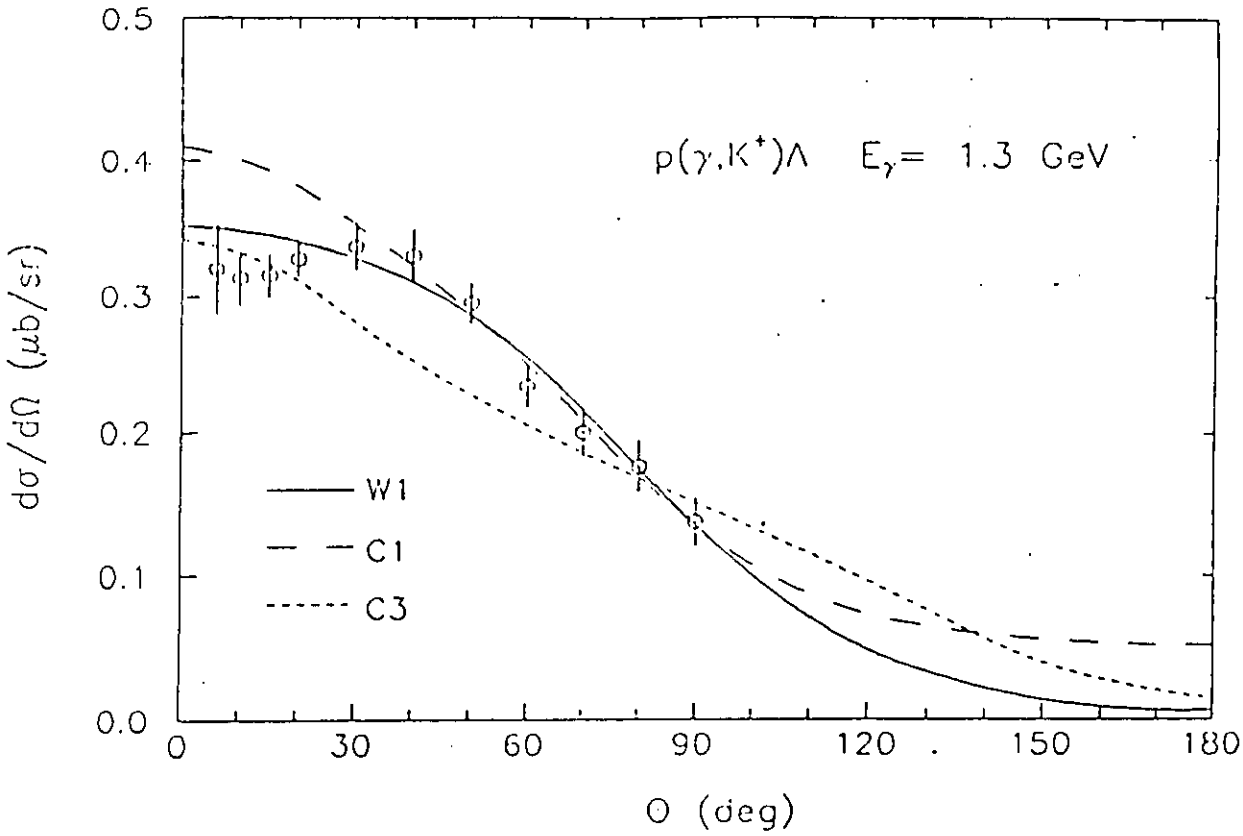
p(γ,K⁺)Λ E_γ= 1.3 GeV
dσ/dΩ (μb/sr)
0.5
0.4
0.3
0.2
0.1
0.0
0
30
60
90
120
150
180
θ (deg)
W1
C1
C3

FIG 2

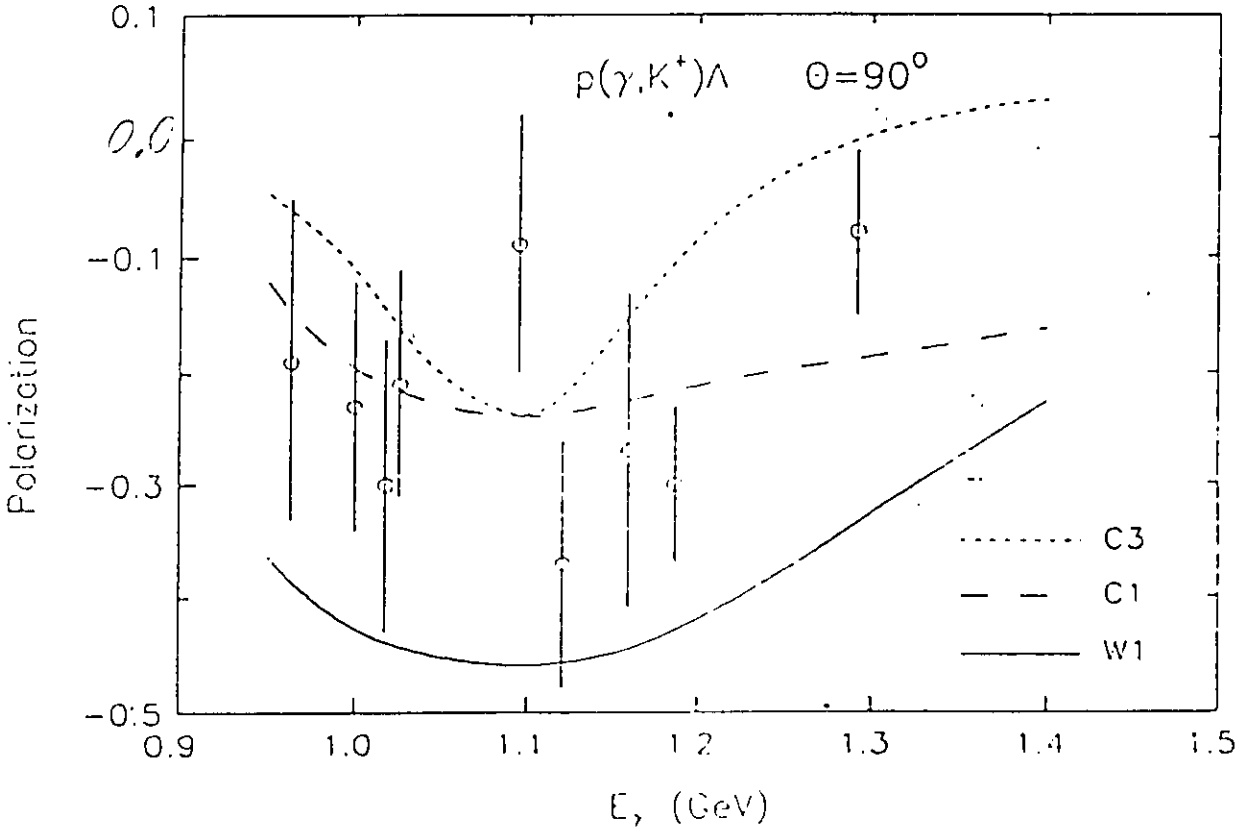
p(γ,K⁺)Λ θ=90°
Polarization
0.1
0.0
-0.1
-0.3
-0.5
0.9
1.0
1.1
1.2
1.3
1.4
1.5
E_γ (GeV)
C3
C1
W1

FIG. 3

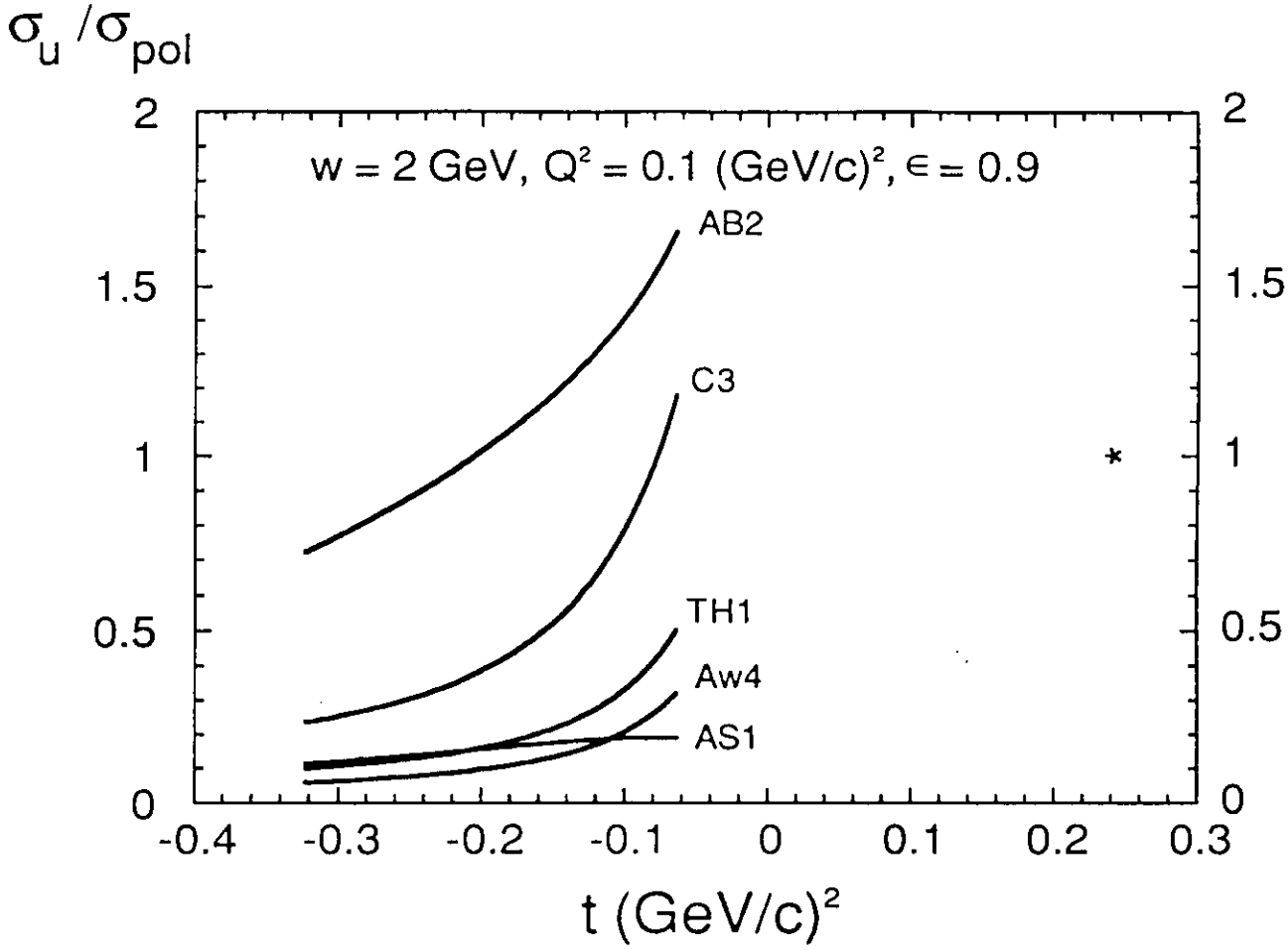
σu /σpol
w = 2 GeV, Q² = 0.1 (GeV/c)², ∈ = 0.9
AB2
C3
TH1
Aw4
AS1
*
2
1.5
1
0.5
0
-0.4
-0.3
-0.2
-0.1
0
0.1
0.2
0.3
t (GeV/c)²

Fig. 5

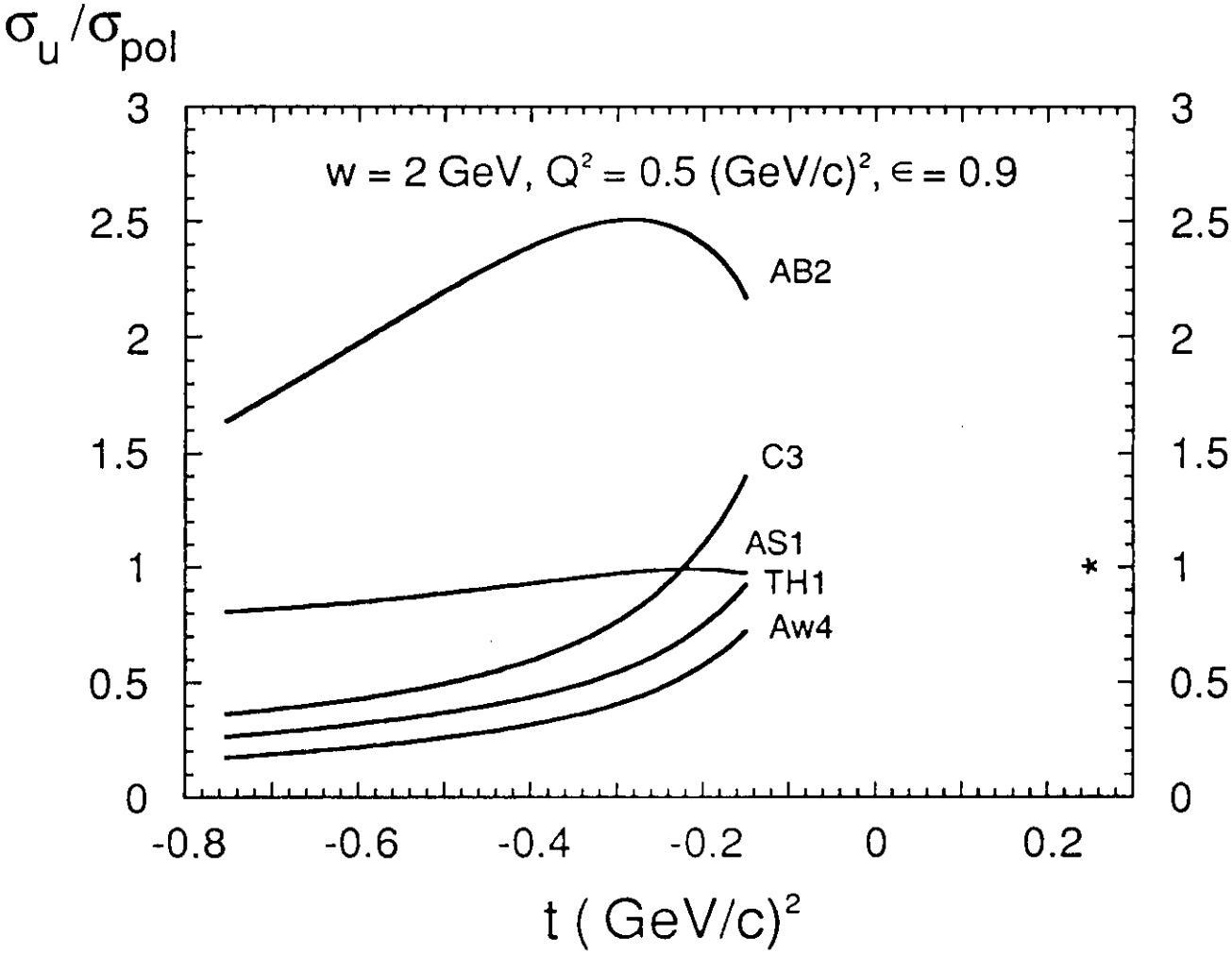
σu /σpol
w = 2 GeV, Q² = 0.5 (GeV/c)², ∈ = 0.9
AB2
C3
AS1
TH1
Aw4
*
3
2.5
2
1.5
1
0.5
0
-0.8
-0.6
-0.4
-0.2
0
0.2
t (GeV/c)²

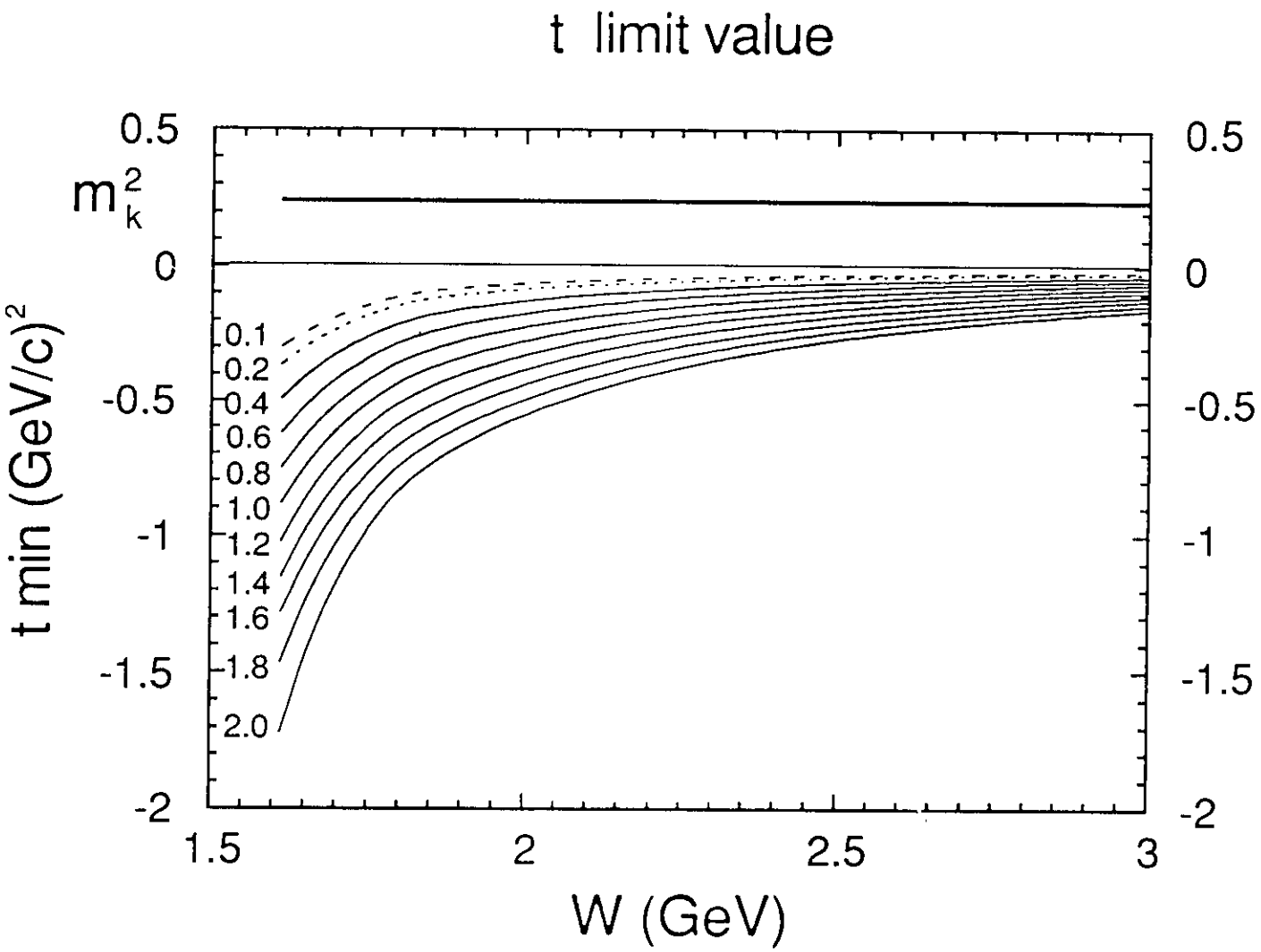
t limit value
0.5
m_k^2
0
-0.5
-1
-1.5
-2
t min (GeV/c)^2
0.1
0.2
0.4
0.6
0.8
1.0
1.2
1.4
1.6
1.8
2.0
1.5
2
2.5
3
W (GeV)

Fig. 4

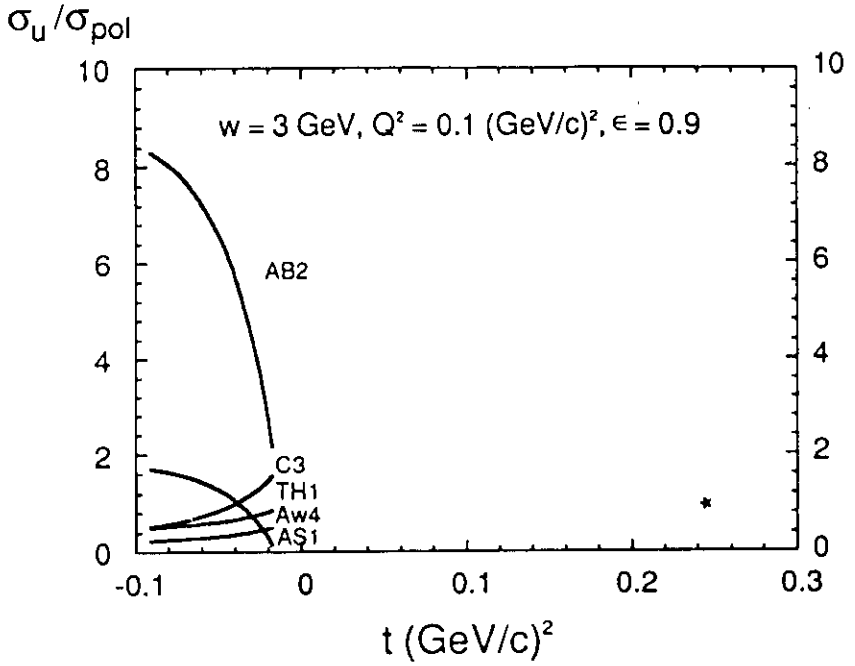

Fig. 7

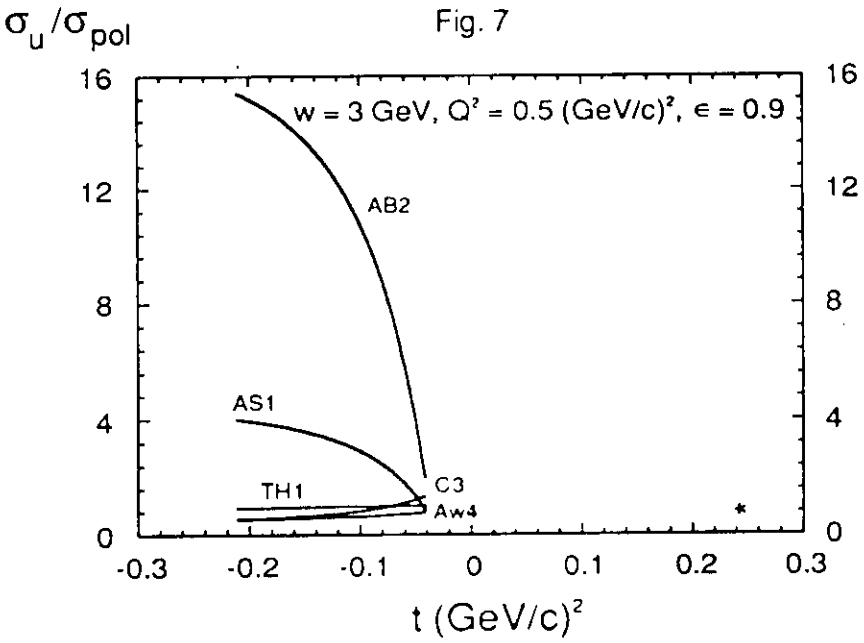

Fig. 8

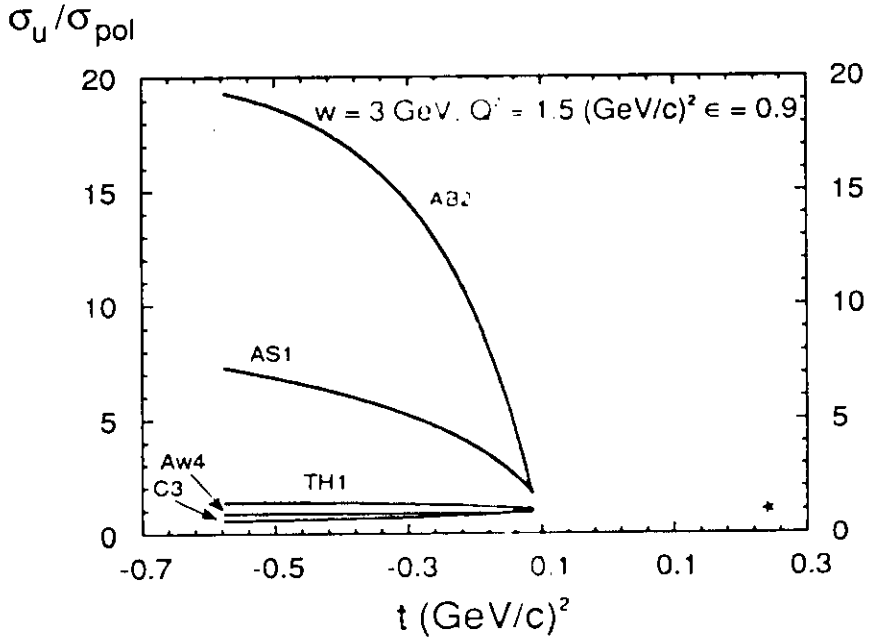

Fig. 9

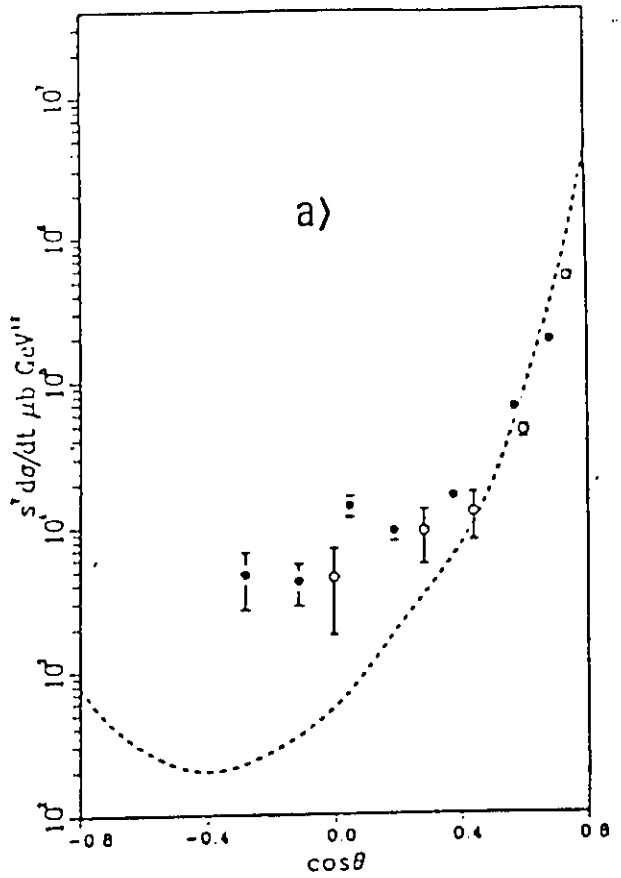
a)
$s^2 d\sigma/dt$ μb GeV^{-4}
cosθ

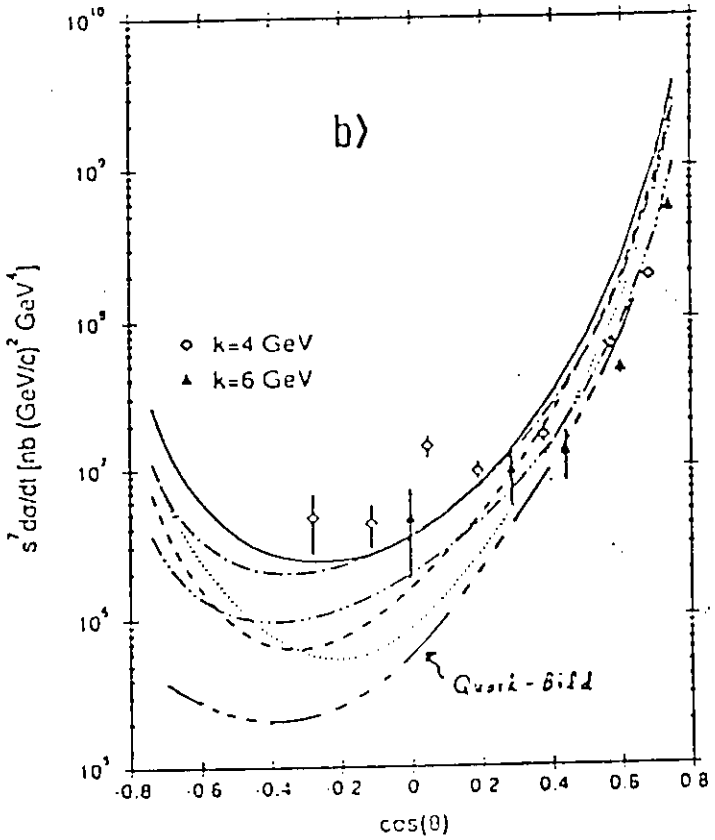
b)
k=4 GeV
k=6 GeV
Quark - Bild
$s^2 d\sigma/dt$ [nb (GeV/c)^2 GeV^4]
cos(θ)

FIG. 10

Kinematics for hypernuclear conditions

TABLE 2

q^2= -0.1 GeV^2	w = 1.9 GeV	t = -0.08GeV^2	p_k = 1.17GeV/c	
E_{in}= 4.112 GeV	E_{out}= 2.604GeV	Θ_e= 5.5 deg	ε = 0.9	
Θk (deg)	Φk (deg)	α (deg)	σ(e,e'k) nb/GeV/sr2	counts/hour
9.4	0.	0.	67.89	7634
Single rate(e,e') (sec^{-1})	Single rate(e,p) (sec^{-1})	Single rate(e,π^+) (sec^{-1})	Single rate(e,k) (sec^{-1})	Accidental rate (e,e'k) (hour^{-1})
1.1 10^5	4.3 10^7	1.0 10^7	1.1 10^3	25
E_{in}= 2.088 GeV	E_{out}= 0.58 GeV	Θ_e= 16.5 deg	ε = 0.5	
Θk (deg)	Φk (deg)	α (deg)	σ(e,e'k) nb/GeV/sr2	counts/hour
6.1	0.	0.	5.47	137
Single rate(e,e') (sec^{-1})	Single rate(e,p) (sec^{-1})	Single rate(e,π^+) (sec^{-1})	Single rate(e,k) (sec^{-1})	Accidental rate (e,e'k) (hour^{-1})
3000	3.12 10^7	7.0 10^6	340	4.6 10^{-2}

beam time and statistical accuracy for the measured cross sections

ε	α	$\delta\sigma$ (%)	**Beam time (hours)**
0.9	0.	1	1.3
0.5	0.	2.	18.2
statistical accuracy for the separated cross sections			
$\delta\sigma$T (%)	$\delta\sigma$L (%)	$\delta\sigma$P (%)	$\delta\sigma$I (%)
5.2	30.4	--	--

TABLE 3

q^2= -0.1 GeV^2	w = 1.9 GeV	t = -0.153 GeV^2	p_k = 1.13GeV/c	
E_{in}= 4.112 GeV	E_{out}= 2.604GeV	Θ_e= 5.5 deg	ε = 0.9	
Θk (deg)	Φk (deg)	α (deg)	σ(e,e'k) nb/GeV/sr2	counts/hour
20.01	0.	0.	44.02	4.94 10^3
6.07	10.09	108.	77.98	8.76 10^3
15.68	8.57	54.	65.70	7.38 10^3
Single rate(e,e') (sec^{-1})	Single rate(e,p) (sec^{-1})	Single rate(e,π^+) (sec^{-1})	Single rate(e,k) (sec^{-1})	Accidental rate (e,e'k) (hour^{-1})
1.1 10^5	4.0 10^7	1.0 10^7	1.0 10^3	25
E_{in}= 2.088 GeV	E_{out}= 0.58 GeV	Θ_e= 16.5 deg	ε = 0.5	
Θk (deg)	Φk (deg)	α (deg)	σ(e,e'k) nb/GeV/sr2	counts/hour
16.76	0.	0.	4.02	100
Single rate(e,e') (sec^{-1})	Single rate(e,p) (sec^{-1})	Single rate(e,π^+) (sec^{-1})	Single rate(e,k) (sec^{-1})	Accidental rate (e,e'k) (hour^{-1})
3.04 10^3	2.98 10^7	6.78 10^6	330	4.6 10^{-2}

beam time and statistical accuracy for the measured cross sections

ε	α	$\delta\sigma$ (%)	Beam time (hours)
0.9	0.	1.	2.0
0.9	108.	1.	1.1
0.9	54.	1.	1.4
0.5	0.	2.	25.0
statistical accuracy for the separated cross sections			
$\delta\sigma$T (%)	$\delta\sigma$L (%)	$\delta\sigma$P (%)	$\delta\sigma$I (%)
4.3	16.8	6.9	30.2

Kinematics for kaon form factor investigations

TABLE 4

q^2= -0.1 GeV^2	w = 2.1 GeV	t = -0.054 GeV^2	p_k = 1.64 GeV/c	
E_{in}= 4.684 GeV	E_{out}= 2.75 GeV	Θ_e= 5.05 deg	ε = 0.87	
Θk (deg)	Φk (deg)	α (deg)	σ(e,e'k) nb/GeV/sr2	counts/hour
7.09	0.	0.	63.3	1.0 10^4
Single rate(e,e') (sec^{-1})	Single rate(e,p) (sec^{-1})	Single rate(e,π^+) (sec^{-1})	Single rate(e,k) (sec^{-1})	Accidental rate (e,e'k) ($hour^{-1}$)
8.0 10^4	4.1 10^7	1.1 10^7	1.7 10^3	4.
E_{in}= 2.735 GeV	E_{out}= 0.498GeV	Θ_e= 12.26 deg	ε = 0.35	
Θk (deg)	Φk (deg)	α (deg)	σ(e,e'k) nb/GeV/sr2	counts/hour
4.98	0.	0.	8.2	378
Single rate(e,e') (sec^{-1})	Single rate(e,p) (sec^{-1})	Single rate(e,π^+) (sec^{-1})	Single rate(e,k) (sec^{-1})	Accidental rate (e,e'k) ($hour^{-1}$)
4.1 10^3	3.1 10^7	8.4 10^6	680	0.09

beam time and statistical accuracy for the measured cross sections

ε	α	$\delta\sigma$ (%)	Beam time (hours)
0.87	0.	1	1
0.35	0.	2.	6.6
statistical accuracy for the separated cross sections			
$\delta\sigma$T (%)	$\delta\sigma$L (%)	$\delta\sigma$P (%)	$\delta\sigma$I (%)
3.2	21.7	--	--

TABLE 5

q^2= -0.1 GeV^2	w = 2.1 GeV	t = -0.257 GeV^2	p_k = 1.53GeV/c	
E_{in}= 4.684 GeV	E_{out}= 2.75 GeV	Θ_e= 5.05 deg	ε = 0.87	
Θk (deg)	Φk (deg)	α (deg)	σ(e,e'k) nb/GeV/sr2	counts/hour
21.08	0.	0.	21.9	3.47 10^3
16.38	10.91	49.	115.0	1.82 10^4
5.11	13.85	98.	187.5	2.97 10^4
Single rate(e,e') (sec^{-1})	Single rate(e,p) (sec^{-1})	Single rate(e,π^+) (sec^{-1})	Single rate(e,k) (sec^{-1})	Accidental rate (e,e'k) ($hour^{-1}$)
8.0 10^4	3.8 10^7	1.1 10^7	1.6 10^3	4.3
E_{in}= 2.538 GeV	E_{out}= 0.604GeV	Θ_e= 14.67 deg	ε = 0.44	
Θk (deg)	Φk (deg)	α (deg)	σ(e,e'k) nb/GeV/sr2	counts/hour
18.47	0.	0.	5.7	198
Single rate(e,e') (sec^{-1})	Single rate(e,p) (sec^{-1})	Single rate(e,π^+) (sec^{-1})	Single rate(e,k) (sec^{-1})	Accidental rate (e,e'k) ($hour^{-1}$)
2.38 10^3	2.79 10^7	7.78 10^6	497	0.04

beam time and statistical accuracy for the measured cross sections

ε	α	$\delta\sigma$ (%)	Beam time (hours)
0.87	0.	1.	2.9
0.87	49.	1.	0.55
0.87	98.	1.	0.3
0.44	0.	2.	12.6
statistical accuracy for the separated cross sections			
$\delta\sigma$T (%)	$\delta\sigma$L (%)	$\delta\sigma$P (%)	$\delta\sigma$I (%)
2.7	37.8	3.	51.4

TABLE 6

q^2= -0.1 GeV^2	w = 2.1 GeV	t = -0.369 GeV^2	p_k = 1.462GeV/c	
E_{in}= 4.684 GeV	E_{out}= 2.75 GeV	Θ_e= 5.05 deg	ε = 0.87	
Θk (deg)	Φk (deg)	α (deg)	σ(e,e'k) nb/GeV/sr2	counts/hour
24.9	0.	0.	16.1	2.55 10^3
19.22	13.14	48.	106.7	1.69 10^4
5.17	18.42	96.	184.8	2.93 10^4
Single rate(e,e') (sec^{-1})	Single rate(e,p) (sec^{-1})	Single rate(e,π^+) (sec^{-1})	Single rate(e,k) (sec^{-1})	Accidental rate (e,e'k) ($hour^{-1}$)
8.0 10^4	3.7 10^7	1.1 10^7	1.6 10^3	4.3
E_{in}= 2.538 GeV	E_{out}= 0.604GeV	Θ_e= 14.67 deg	ε = 0.44	
Θk (deg)	Φk (deg)	α (deg)	σ(e,e'k) nb/GeV/sr2	counts/hour
22.29	0.	0.	5.3	198
Single rate(e,e') (sec^{-1})	Single rate(e,p) (sec^{-1})	Single rate(e,π^+) (sec^{-1})	Single rate(e,k) (sec^{-1})	Accidental rate (e,e'k) ($hour^{-1}$)
2.38 10^3	2.72 10^7	7.45 10^6	417	0.035

beam time and statistical accuracy for the measured cross sections

ε	α	$\delta\sigma$ (%)	Beam time (hours)
0.87	0.	1.	2.9
0.87	48.	1.	0.55
0.87	96.	1.	0.3
0.44	0.	2.	12.6
statistical accuracy for the separated cross sections			
$\delta\sigma$T (%)	$\delta\sigma$L (%)	$\delta\sigma$P (%)	$\delta\sigma$I (%)
2.6	45.4	3.	41.

TABLE 7

q^2= -0.1 GeV^2	w = 2.1 GeV	t = -0.595 GeV^2	p_k = 1.335GeV/c	
E_{in}= 4.684 GeV	E_{out}= 2.75 GeV	Θ_e= 5.05 deg	ε = 0.87	
Θk (deg)	Φk (deg)	α (deg)	σ(e,e'k) nb/GeV/sr2	counts/hour
31.45	0.	0.	11.4	1.8 10^3
24.25	17.55	47.	75.8	1.20 10^4
5.29	24.29	94.	137.6	2.18 10^4
Single rate(e,e') (sec^{-1})	Single rate(e,p) (sec^{-1})	Single rate(e,π^+) (sec^{-1})	Single rate(e,k) (sec^{-1})	Accidental rate (e,e'k) ($hour^{-1}$)
8.0 10^4	3.5 10^7	1.0 10^7	1.4 10^3	4.4
E_{in}= 2.538 GeV	E_{out}= 0.604GeV	Θ_e= 14.67 deg	ε = 0.44	
Θk (deg)	Φk (deg)	α (deg)	σ(e,e'k) nb/GeV/sr2	counts/hour
28.83	0.	0.	4.0	139
Single rate(e,e') (sec^{-1})	Single rate(e,p) (sec^{-1})	Single rate(e,π^+) (sec^{-1})	Single rate(e,k) (sec^{-1})	Accidental rate (e,e'k) ($hour^{-1}$)
2.38 10^3	2.56 10^7	1.04 10^7	435	0.04

beam time and statistical accuracy for the measured cross sections

ε	α	$\delta\sigma$ (%)	Beam time (hours)
0.87	0.	1.	5.6
0.87	47.	1.	0.8
0.87	94.	1.	0.5
0.44	0.	2.	18.0
statistical accuracy for the separated cross sections			
$\delta\sigma$T (%)	$\delta\sigma$L (%)	$\delta\sigma$P (%)	$\delta\sigma$I (%)
2.6	65.9	3.2	30.9

TABLE 8

q^2= -0.3 GeV^2	w = 2.2 GeV	t = -0.075GeV^2	p_k = 1.975GeV/c	
E_{in}= 5.974 GeV	E_{out}= 3.705GeV	Θ_e= 6.67 deg	ε = 0.89	
Θk (deg)	Φk (deg)	α (deg)	σ(e,e'k) nb/GeV/sr2	counts/hour
10.63	0.	0.	22.9	5863
Single rate(e,e') (sec^{-1})	Single rate(e,p) (sec^{-1})	Single rate(e,π^+) (sec^{-1})	Single rate(e,k) (sec^{-1})	Accidental rate (e,e'k) (hour^{-1})
2.4 10^4	4.3 10^7	1.3 10^7	2.8 10^3	1.6
E_{in}= 2.877 GeV	E_{out}= 0.607 GeV	Θ_e= 23.92 deg	ε = 0.38	
Θk (deg)	Φk (deg)	α (deg)	σ(e,e'k) nb/GeV/sr2	counts/hour
6.05	0.	0.	1.1	180.
Single rate(e,e') (sec^{-1})	Single rate(e,p) (sec^{-1})	Single rate(e,π^+) (sec^{-1})	Single rate(e,k) (sec^{-1})	Accidental rate (e,e'k) (hour^{-1})
1.2 10^3	3.0 10^7	8.3 10^6	674	2.1 10^{-2}

beam time and statistical accuracy for the measured cross sections

ε	α	$\delta\sigma$ (%)	**Beam time (hours)**
0.89	0.	1	1.7
0.38	0.	1	55.5
statistical accuracy for the separated cross sections			
$\delta\sigma$T (%)	$\delta\sigma$L (%)	$\delta\sigma$P (%)	$\delta\sigma$I (%)
2.6	5.3	--	--

TABLE 9

q^2= -0.3 GeV^2	w = 2.2 GeV	t = -0.218GeV^2	p_k = 1.896GeV/c	
E_{in}= 5.974 GeV	E_{out}= 3.705GeV	Θ_e= 6.67 deg	ε = 0.89	
Θk (deg)	Φk (deg)	α (deg)	σ(e,e'k) nb/GeV/sr2	counts/hour
20.14	0.	0.	12.5	3.2 10^3
15.42	8.23	60.	70.7	1.8 10^4
5.83	8.23	120.	75.2	1.9 10^4
Single rate(e,e') (sec^{-1})	Single rate(e,p) (sec^{-1})	Single rate(e,π^+) (sec^{-1})	Single rate(e,k) (sec^{-1})	Accidental rate (e,e'k) (hour^{-1})
2.4 10^4	4.3 10^7	1.3 10^7	2.6 10^3	1.6
E_{in}= 2.877 GeV	E_{out}= 0.607 GeV	Θ_e= 23.92 deg	ε = 0.38	
Θk (deg)	Φk (deg)	α (deg)	σ(e,e'k) nb/GeV/sr2	counts/hour
15.57	0.	0.	1.9	311.
Single rate(e,e') (sec^{-1})	Single rate(e,p) (sec^{-1})	Single rate(e,π^+) (sec^{-1})	Single rate(e,k) (sec^{-1})	Accidental rate (e,e'k) (hour^{-1})
1.2 10^3	2.8 10^7	8.5 10^6	647	2.1 10^{-2}

beam time and statistical accuracy for the measured cross sections

ε	α	$\delta\sigma$ (%)	**Beam time (hours)**
0.89	0.	1	3.1
0.89	60.	1	0.6
0.89	120.	1	0.5
0.38	0.	1	32.2
statistical accuracy for the separated cross sections			
$\delta\sigma$T (%)	$\delta\sigma$L (%)	$\delta\sigma$P (%)	$\delta\sigma$I (%)
1.3	8.2	2.0	23.1

TABLE 10

q^2= -0.3 GeV^2	w = 2.2 GeV	t = -0.390GeV^2	p_k = 1.802GeV/c	
E_{in}= 5.974 GeV	E_{out}= 3.705GeV	Θ_e= 6.67 deg	ε = 0.89	
Θk (deg)	Φk (deg)	α (deg)	σ(e,e'k) nb/GeV/sr2	counts/hour
25.1	0.	0.	7.8	1.8 10^3
19.05	11.81	55.	74.1	1.7 10^4
5.58	13.58	110.	101.2	2.4 10^4
Single rate(e,e') (sec^{-1})	Single rate(e,p) (sec^{-1})	Single rate(e,π^+) (sec^{-1})	Single rate(e,k) (sec^{-1})	Accidental rate (e,e'k) ($hour^{-1}$)
2.4 10^4	4.2 10^7	1.3 10^7	2.3 10^3	1.5
E_{in}= 2.877 GeV	E_{out}= 0.607 GeV	Θ_e= 23.92 deg	ε = 0.38	
Θk (deg)	Φk (deg)	α (deg)	σ(e,e'k) nb/GeV/sr2	counts/hour
20.52	0.	0.	2.1	343.
Single rate(e,e') (sec^{-1})	Single rate(e,p) (sec^{-1})	Single rate(e,π^+) (sec^{-1})	Single rate(e,k) (sec^{-1})	Accidental rate (e,e'k) ($hour^{-1}$)
1.2 10^3	2.8 10^7	8.1 10^6	615	2.1 10^{-2}

beam time and statistical accuracy for the measured cross sections

ε	α	$\delta\sigma$ (%)	**Beam time (hours)**
0.89	0.	1	5.6
0.89	60.	1	0.6
0.89	120.	1	0.4
0.38	0.	1	29.2
statistical accuracy for the separated cross sections			
$\delta\sigma$T (%)	$\delta\sigma$L (%)	$\delta\sigma$P (%)	$\delta\sigma$I (%)
1.3	13.7	2.2	23.2

TABLE 11

q^2= -0.3 GeV^2	w = 2.2 GeV	t = -0.591GeV^2	p_k = 1.690GeV/c	
E_{in}= 5.974 GeV	E_{out}= 3.705GeV	Θ_e= 6.67 deg	ε = 0.89	
Θk (deg)	Φk (deg)	α (deg)	σ(e,e'k) nb/GeV/sr2	counts/hour
29.71	0.	0.	5.7	1.3 10^3
22.39	15.14	53.	62.8	1.5 10^4
5.51	18.41	105.	95.0	2.2 10^4
Single rate(e,e') (sec^{-1})	Single rate(e,p) (sec^{-1})	Single rate(e,π^+) (sec^{-1})	Single rate(e,k) (sec^{-1})	Accidental rate (e,e'k) (hour^{-1})
2.4 10^4	4.0 10^7	1.3 10^7	2.2 10^3	1.5
E_{in}= 2.877 GeV	E_{out}= 0.607 GeV	Θ_e= 23.92 deg	ε = 0.38	
Θk (deg)	Φk (deg)	α (deg)	σ(e,e'k) nb/GeV/sr2	counts/hour
25.14	0.	0.	1.9	285.
Single rate(e,e') (sec^{-1})	Single rate(e,p) (sec^{-1})	Single rate(e,π^+) (sec^{-1})	Single rate(e,k) (sec^{-1})	Accidental rate (e,e'k) (hour^{-1})
1.2 10^3	2.5 10^7	8.1 10^6	528.	1.9 10^{-2}

beam time and statistical accuracy for the measured cross sections

ε	α	$\delta\sigma$ (%)	Beam time (hours)
0.89	0.	1	7.7
0.89	60.	1	0.7
0.89	120.	1	0.45
0.38	0.	1	35.1
statistical accuracy for the separated cross sections			
$\delta\sigma$T (%)	$\delta\sigma$L (%)	$\delta\sigma$P (%)	$\delta\sigma$I (%)
1.4	19.2	2.4	23.4

TABLE 12

q^2= -0.5 GeV^2	w = 2.2 GeV	t = -0.107 GeV^2	p_k = 2.067GeV/c	
E_{in}= 6.095 GeV	E_{out}= 3.719 GeV	Θ_e= 8.5 deg	ε = 0.88	
Θk (deg)	Φk (deg)	α (deg)	σ(e,e'k) nb/GeV/sr2	counts/hour
12.83	0.	0.	10.4	2.45 10^3
Single rate(e,e') (sec^{-1})	Single rate(e,p) (sec^{-1})	Single rate(e,π^+) (sec^{-1})	Single rate(e,k) (sec^{-1})	Accidental rate (e,e'k) ($hour^{-1}$)
9.4 10^3	4.3 10^7	1.4 10^7	2.6 10^3	0.6
E_{in}= 2.975 GeV	E_{out}= 0.598GeV	Θ_e= 30.7 deg	ε = 0.35	
Θk (deg)	Φk (deg)	α (deg)	σ(e,e'k) nb/GeV/sr2	counts/hour
7.08	0.	0.	0.4	59
Single rate(e,e') (sec^{-1})	Single rate(e,p) (sec^{-1})	Single rate(e,π^+) (sec^{-1})	Single rate(e,k) (sec^{-1})	Accidental rate (e,e'k) ($hour^{-1}$)
4.6 10^2	2.91 10^7	8.68 10^6	612	6.5 10^{-3}

beam time and statistical accuracy for the measured cross sections

ε	α	$\delta\sigma$ (%)	Beam time (hours)
0.88	0.	1.	4.1
0.35	0.	2.5	27.1
statistical accuracy for the separated cross sections			
$\delta\sigma$T (%)	$\delta\sigma$L (%)	$\delta\sigma$P (%)	$\delta\sigma$I (%)
6.9	5.1	--	--

TABLE 13

q^2= -0.5 GeV^2	w = 2.2 GeV	t = -0.228 GeV^2	p_k = 2.000GeV/c	
E_{in}= 6.095 GeV	E_{out}= 3.719 GeV	Θ_e= 8.5 deg	ε = 0.88	
Θk (deg)	Φk (deg)	α (deg)	σ(e,e'k) nb/GeV/sr2	counts/hour
20.94	0.	0.	6.6	1.5510^3
14.94	7.82	75.	35.1	8.2610^3
5.81	4.04	150.	18.1	4.2510^3
Single rate(e,e') (sec^{-1})	Single rate(e,p) (sec^{-1})	Single rate(e,π^+) (sec^{-1})	Single rate(e,k) (sec^{-1})	Accidental rate (e,e'k) ($hour^{-1}$)
$9.4\ 10^3$	$4.2\ 10^7$	$1.3\ 10^7$	$2.5\ 10^3$	0.55
E_{in}= 2.975 GeV	E_{out}= 0.598GeV	Θ_e= 30.7 deg	ε = 0.35	
Θk (deg)	Φk (deg)	α (deg)	σ(e,e'k) nb/GeV/sr2	counts/hour
15.19	0.	0.	0.8	118
Single rate(e,e') (sec^{-1})	Single rate(e,p) (sec^{-1})	Single rate(e,π^+) (sec^{-1})	Single rate(e,k) (sec^{-1})	Accidental rate (e,e'k) ($hour^{-1}$)
$4.6\ 10^2$	$2.9\ 10^7$	$8.7\ 10^6$	612	$6.5\ 10^{-3}$

beam time and statistical accuracy for the measured cross sections

ε	α	$\delta\sigma$ (%)	Beam time (hours)
0.88	0.	1.	6.5
0.88	75.	1.	1.2
0.88	150.	1.	2.4
0.35	0.	2.	21.2
statistical accuracy for the separated cross sections			
$\delta\sigma$T (%)	$\delta\sigma$L (%)	$\delta\sigma$P (%)	$\delta\sigma$I (%)
2.4	9.1	1.5	5.4

TABLE 14

q^2= -0.5 GeV^2	w = 2.2 GeV	t = -0.411 GeV^2	p_k = 1.900GeV/c	
E_{in}= 6.095 GeV	E_{out}= 3.719 GeV	Θ_e= 8.5 deg	ε = 0.88	
Θk (deg)	Φk (deg)	α (deg)	σ(e,e'k) nb/GeV/sr2	counts/hour
25.97	0.	0.	4.2	9.4310^2
18.88	11.68	63.	39.3	8.810^3
5.21	10.72	125.	38.2	8.610^3
Single rate(e,e') (sec^{-1})	Single rate(e,p) (sec^{-1})	Single rate(e,π^+) (sec^{-1})	Single rate(e,k) (sec^{-1})	Accidental rate (e,e'k) ($hour^{-1}$)
$9.4\ 10^3$	$4.3\ 10^7$	$1.3\ 10^7$	$2.2\ 10^3$	0.55
E_{in}= 2.975 GeV	E_{out}= 0.598GeV	Θ_e= 30.7 deg	ε = 0.35	
Θk (deg)	Φk (deg)	α (deg)	σ(e,e'k) nb/GeV/sr2	counts/hour
20.21	0.	0.	1.0	36
Single rate(e,e') (sec^{-1})	Single rate(e,p) (sec^{-1})	Single rate(e,π^+) (sec^{-1})	Single rate(e,k) (sec^{-1})	Accidental rate (e,e'k) ($hour^{-1}$)
$4.6\ 10^2$	$2.7\ 10^7$	$8.5\ 10^6$	537	$6.5\ 10^{-3}$

beam time and statistical accuracy for the measured cross sections

ε	α	$\delta\sigma$ (%)	Beam time (hours)
0.88	0.	1.	10.6
0.88	63.	1.	1.1
0.88	125.	1.	1.2
0.35	0.	2.	17.7
statistical accuracy for the separated cross sections			
$\delta\sigma$T (%)	$\delta\sigma$L (%)	$\delta\sigma$P (%)	$\delta\sigma$I (%)
2.2	17.0	1.8	11.7

TABLE 15

q^2= -0.5 GeV^2	w = 2.2 GeV	t = -0.594 GeV^2	p_k = 1.800GeV/c	
E_{in}= 6.095 GeV	E_{out}= 3.719 GeV	Θ_e= 8.5 deg	ε = 0.88	
Θk (deg)	Φk (deg)	α (deg)	σ(e,e'k) nb/GeV/sr2	counts/hour
29.88	0.	0.	3.1	6.910^2
22.06	14.39	58.	34.0	7.610^3
5.45	15.41	115.	42.1	9.510^3
Single rate(e,e') (sec^{-1})	Single rate(e,p) (sec^{-1})	Single rate(e,π^+) (sec^{-1})	Single rate(e,k) (sec^{-1})	Accidental rate (e,e'k) ($hour^{-1}$)
9.4 10^3	4.0 10^7	1.3 10^7	2.1 10^3	0.55
E_{in}= 2.975 GeV	E_{out}= 0.598GeV	Θ_e= 30.7 deg	ε = 0.35	
Θk (deg)	Φk (deg)	α (deg)	σ(e,e'k) nb/GeV/sr2	counts/hour
24.13	0.	0.	0.9	127
Single rate(e,e') (sec^{-1})	Single rate(e,p) (sec^{-1})	Single rate(e,π^+) (sec^{-1})	Single rate(e,k) (sec^{-1})	Accidental rate (e,e'k) ($hour^{-1}$)
4.6 10^2	2.7 10^7	8.1 10^6	508	6.5 10^{-3}

beam time and statistical accuracy for the measured cross sections

ε	α	$\delta\sigma$ (%)	**Beam time (hours)**
0.88	0.	1.	14.5
0.88	58.	1.	1.3
0.88	115.	1.	1.1
0.35	0.	2.	19.7

statistical accuracy for the separated cross sections

$\delta\sigma$T (%)	$\delta\sigma$L (%)	$\delta\sigma$P (%)	$\delta\sigma$I (%)
2.2	13.8	2.04	15.4

TABLE 17

q^2= -1.0 GeV^2	w = 2.236 GeV	t = -0.804GeV^2	p_k = 2.047GeV/c	
E_{in}= 5.984 GeV	E_{out}= 3.256GeV	Θ_e= 13. deg	ε = 0.82	
Θk (deg)	Φk (deg)	α (deg)	σ(e,e'k) nb/GeV/sr2	counts/hour
30.49	0.	0.	1.1	1.0 10^3
23.18	13.42	58.	8.2	7.5 10^3
10.40	15.33	105.	10.9	1.0 10^4
Single rate(e,e') (sec^{-1})	Single rate(e,p) (sec^{-1})	Single rate(e,π^+) (sec^{-1})	Single rate(e,k) (sec^{-1})	Accidental rate (e,e'k) (hour^{-1})
6.2 10^3	4.0 10^7	1.3 10^7	2.4 10^3	0.36
E_{in}= 3.344 GeV	E_{out}= 0.616 GeV	Θ_e= 40.8 deg	ε = 0.3	
Θk (deg)	Φk (deg)	α (deg)	σ(e,e'k) nb/GeV/sr2	counts/hour
23.84	0.	0.	0.4	69.
Single rate(e,e') (sec^{-1})	Single rate(e,p) (sec^{-1})	Single rate(e,π^+) (sec^{-1})	Single rate(e,k) (sec^{-1})	Accidental rate (e,e'k) (hour^{-1})
97.	2.8 10^7	9.2 10^6	625	1.4 10^{-3}

beam time and statistical accuracy for the measured cross sections

ε	α	$\delta\sigma$ (%)	Beam time (hours)
0.82	0.	1.	10.
0.82	58.	1.	1.3
0.82	105.	1.	1.
0.3	0.	3.	16.
statistical accuracy for the separated cross sections			
$\delta\sigma$T (%)	$\delta\sigma$L (%)	$\delta\sigma$P (%)	$\delta\sigma$I (%)
3.3	31.3	2.7	25.0

Large t kinematics

TABLE 16

q^2= -1.0 GeV^2	w = 2.236 GeV	t = -0.186GeV^2	p_k = 2.385GeV/c	
E_{in}= 5.984 GeV	E_{out}= 3.256GeV	Θ_e= 13. deg	ε = 0.82	
Θk (deg)	Φk (deg)	α (deg)	σ(e,e'k) nb/GeV/sr2	counts/hour
14.61	0.	0.	2.3	2102
Single rate(e,e') (sec^{-1})	Single rate(e,p) (sec^{-1})	Single rate(e,π^+) (sec^{-1})	Single rate(e,k) (sec^{-1})	Accidental rate (e,e'k) (hour^{-1})
6.2 10^3	4.1 10^7	1.4 10^7	2.8 10^3	0.36
E_{in}= 3.344 GeV	E_{out}= 0.616 GeV	Θ_e= 40.8 deg	ε = 0.3	
Θk (deg)	Φk (deg)	α (deg)	σ(e,e'k) nb/GeV/sr2	counts/hour
7.96	0.	0.	0.1	17.3
Single rate(e,e') (sec^{-1})	Single rate(e,p) (sec^{-1})	Single rate(e,π^+) (sec^{-1})	Single rate(e,k) (sec^{-1})	Accidental rate (e,e'k) (hour^{-1})
97.	3.0 10^7	9.3 10^6	728	1.4 10^{-3}

beam time and statistical accuracy for the measured cross sections

ε	α	$\delta\sigma$ (%)	**Beam time (hours)**
0.82	0.	2.	1.2
0.3	0.	3.	64.2
statistical accuracy for the separated cross sections			
$\delta\sigma$T (%)	$\delta\sigma$L (%)	$\delta\sigma$P (%)	$\delta\sigma$I (%)
11.	3.7	--	--

TABLE 19

q^2= -1.0 GeV^2	w = 2.236 GeV	t = -1.968GeV^2	pk = 1.401GeV/c	
E_{in}= 5.984 GeV	E_{out}= 3.256GeV	Θ_e= 13. deg	ε = 0.82	
Θk (deg)	Φk (deg)	α (deg)	σ(e,e'k) nb/GeV/sr2	counts/hour
44.75	0.	0.	0.3	219.
37.01	23.67	49.	1.9	1.4 10^3
10.23	31.87	97.	3.2	2.3 10^3
Single rate(e,e') (sec^{-1})	Single rate(e,p) (sec^{-1})	Single rate(e,π^+) (sec^{-1})	Single rate(e,k) (sec^{-1})	Accidental rate (e,e'k) (hour^{-1})
6.2 10^3	3.7 10^7	1.2$10^7$	1.6 10^3	0.31
E_{in}= 3.344 GeV	E_{out}= 0.616 GeV	Θ_e= 40.8 deg	ε = 0.3	
Θk (deg)	Φk (deg)	α (deg)	σ(e,e'k) nb/GeV/sr2	counts/hour
40.10	0.	0.	0.1	14.
Single rate(e,e') (sec^{-1})	Single rate(e,p) (sec^{-1})	Single rate(e,π^+) (sec^{-1})	Single rate(e,k) (sec^{-1})	Accidental rate (e,e'k) (hour^{-1})
97.	2.4$10^7$	8.0 10^6	342	1.2 10^{-3}

beam time and statistical accuracy for the measured cross sections

ε	α	$\delta\sigma$ (%)	Beam time (hours)
0.82	0.	1.	45.7
0.82	49.	1.	7.1
0.82	97.	1.	4.3
0.3	0.	3.	79.4
statistical accuracy for the separated cross sections			
$\delta\sigma$T (%)	$\delta\sigma$L (%)	$\delta\sigma$P (%)	$\delta\sigma$I (%)
3.3	46.5	3.2	23.2

TABLE 18

q^2= -1.0 GeV^2	w = 2.236 GeV	t = -1.495GeV^2	pk = 1.666GeV/c	
E_{in}= 5.984 GeV	E_{out}= 3.256GeV	Θ_e= 13. deg	ε = 0.82	
Θk (deg)	Φk (deg)	α (deg)	σ(e,e'k) nb/GeV/sr2	counts/hour
40.05	0.	0.	0.6	460.
31.61	19.22	50.	3.6	2.8 10^3
9.89	25.03	100.	6.0	4.6 10^3
Single rate(e,e') (sec^{-1})	Single rate(e,p) (sec^{-1})	Single rate(e,π^+) (sec^{-1})	Single rate(e,k) (sec^{-1})	Accidental rate (e,e'k) (hour^{-1})
6.2 10^3	3.7 10^7	1.2$10^7$	1.6 10^3	0.31
E_{in}= 3.344 GeV	E_{out}= 0.616 GeV	Θ_e= 40.8 deg	ε = 0.3	
Θk (deg)	Φk (deg)	α (deg)	σ(e,e'k) nb/GeV/sr2	counts/hour
33.44	0.	0.	0.2	29.
Single rate(e,e') (sec^{-1})	Single rate(e,p) (sec^{-1})	Single rate(e,π^+) (sec^{-1})	Single rate(e,k) (sec^{-1})	Accidental rate (e,e'k) (hour^{-1})
97.	2.5 10^7	8.5 10^6	427	1.2 10^{-3}

beam time and statistical accuracy for the measured cross sections

ε	α	$\delta\sigma$ (%)	Beam time (hours)
0.82	0.	1.	21.7
0.82	50.	1.	3.6
0.82	100.	1.	2.2
0.3	0.	3.	38.3
statistical accuracy for the separated cross sections			
$\delta\sigma$T (%)	$\delta\sigma$L (%)	$\delta\sigma$P (%)	$\delta\sigma$I (%)
3.3	46.0	2.3	25.0